Near-Optimal and Suboptimal Receivers for Multiuser UWB Impulse Radio Systems in Multipath

Dong In Kim, *Senior Member, IEEE*

***Abstract*—In this paper, near-optimal and suboptimal receivers are proposed for multiuser ultra-wideband (UWB) impulse radio (IR) systems in dense multipath channels, where *non-Gaussian* multiuser interference (MUI) seen at each finger of a Rake receiver is taken into account. The receivers exploit two-dimensional diversity that is offered by UWB signaling, namely multipath diversity and repetition diversity (i.e., repetition coding). Non-Gaussian modeling of the MUI results in employing a nonlinear process at each finger, jointly considering the desired user's path gain being estimated and the order associated with MUI statistics. For this, the MUI statistics are characterized in terms of their second and fourth order moments, especially considering the channel *sparseness* and *cluster overlapping* observed in realistic UWB channels, which leads to modeling the MUI by a *generalized* Gaussian distribution. It is shown that the MUI statistics exhibit non-Gaussian nature even for relatively large number of users, and the diversity gain against MUI can be significant when relatively small number of users coexist.**

***Index Terms*—Ultra-wideband (UWB), impulse radio (IR), multipath diversity, repetition diversity, multiuser interference (MUI), generalized Gaussian distribution, nonlinear process.**

I. Introduction

RECENTLY, ultra-wideband impulse radio (UWB-IR) technology has gained much attention due to the availability of low-cost and low-power wireless devices for indoor wireless communications, as well as location and ranging purpose, being standardized to the IEEE 802.15.4a [1]. The UWB-IR systems considered time-hopping (TH) multiple access for supporting multiuser access, along with very narrow-width pulse transmission with low duty cycle [2], [3]. In this scenario, the authors have analyzed the multiuser performance by simply invoking the Gaussian approximation for the multiuser interference (MUI). But, recent contributions to the MUI analysis reported in [4]-[8] confirmed that the Gaussian approximation is not accurate enough to predict the multiuser performance. More recent contribution [9] has further clarified this by showing that the impulsive nature of UWB-IR signals is not well mitigated for relatively large number of users.

Paper approved by L. Yang, the Editor for Ultra Wideband of the IEEE Communications Society. Manuscript received October 12, 2007; revised June 27, 2008.

D. I. Kim is with the School of Information and Communication Engineering, Sungkyunkwan University, Suwon 440-746, Korea (e-mail: dikim@ece.skku.ac.kr).

This work was supported by the MIC (Ministry of Information and Communication), Korea, under the ITRC (Information Technology Research Center) support program supervised by the IITA (Institute of Information Technology Assessment) (IITA-2009-C1090-0902-0005).

Digital Object Identifier 10.1109/TCOMM.2009.10.070528

The above observation has motivated an optimal receiver design for multiuser UWB-IR systems, one hand modeling the MUI as a Laplace distribution [10] and a *generalized* Gaussian distribution [11], the other hand modeling it to be a Gaussian *mixture* [12], as a weighted sum of several Gaussian densities with unequal individual variances. They showed that the multiuser performance of UWB-IR systems can be improved significantly compared to conventional single-user detector based on the Gaussian-modeled MUI. Further, this approach has been extended to designing a Rake receiver for use in multipath UWB channels, exploiting the *non-Gaussian* nature of the MUI seen at each finger, that results in improved diversity gain against the MUI, as shown in [13] and [14]. However, the analyses here simply assumed specific channel conditions in modeling the MUI statistics seen at each finger, without considering realistic UWB channel conditions [15].

In this paper, the MUI statistics seen at each finger are evaluated analytically, in terms of the second and fourth order moments, considering the channel *sparseness* and *cluster overlapping*. The sparseness of the UWB channel indicates that there could be no multipath arrival in a time bin, which largely affects the energy capture as well as the MUI across fingers at *partial*-Rake receiver. Moreover, the realistic UWB channels exhibit clustered multipath arrival patterns with possible overlap among them, that also affects the MUI statistics, especially for non-line-of-sight (NLOS) channels. To design practical near-optimal and suboptimal receivers for multiuser UWB-IR systems, generalized Gaussian (GG) distribution is adopted, thereby the second and fourth order moments drived under realistic UWB channels can be used to effectively model the MUI statistics. Especially, the non-Gaussian modeling of the MUI results in employing a nonlinear process at each finger, hence the order of *nonlinearity* needed is theoretically determined under the GG distribution.

The rest of the paper is organized as follows. In Section II, signaling for a multiuser UWB-IR system is described, along with realistic UWB channel model. The MUI statistics are characterized in Section III to evaluate their second and fourth order moments, by which a proper form of nonlinear processing is determined. In Section IV, the analytical results on the MUI statistics are validated through simulations, and then the diversity gain against the MUI is illustrated for near-optimal and suboptimal processing. Concluding remarks are given in Section V.

II. Signal Model

A multiuser UWB-IR system is considered, where the kth ($k = 1, 2, \ldots, K$) user's signal is expressed by

$$s_{tr}^{(k)}(t) = \sqrt{\frac{E_k}{N_s}} \sum_{j=-\infty}^{\infty} d_j^{(k)} b_{\lfloor j/N_s \rfloor}^{(k)} w_{tr}(t - jT_f - c_j^{(k)} T_c). \quad (1)$$

Here, $w_{tr}(t)$ is the unit-energy transmitted pulse of duration T_w, E_k is the symbol energy of user k, T_f is the frame time, N_s is the number of frames used to transmit one information symbol, and $b_i^{(k)}$ is the ith binary information symbol transmitted by user k, taking on the values of $\{-1, 1\}$ with equal probability ($i = \lfloor j/N_s \rfloor$ denotes the integer part of j/N_s). To shape the transmit signal spectrum according to the FCC spectral mask, and to achieve time-hopping (TH) multiple access, the two user-specific sequences are employed, one of which is the pseudorandom sequence $\{d_j^{(k)}\}$ of values ± 1, and the other is the TH code $\{c_j^{(k)}\}$ with elements taking the integer values, i.e., $c_j^{(k)} \in \{0, 1, \ldots, N_h - 1\}$ for the maximum TH shift N_h. Here, the frame time T_f is assumed fixed for all users and meets the constraint $T_f \geq T_{mds} + N_h T_c$ to avoid inter-frame interference (IFI), where T_c denotes the chip time with $T_c \geq T_w$ and T_{mds} represents the channel delay spread.

A K-user asynchronous transmission along with multipath fading is modeled as

$$h^{(k)}(t - \tau^{(k)}) = \sum_{l=0}^{L-1} a_l^{(k)} \delta(t - \tau^{(k)} - l\Delta) \quad (2)$$

where L is the number of multipaths, $a_l^{(k)}$ is the channel gain of lth path of kth user, $\tau^{(k)}$ is the asynchronous delay of kth user, uniformly distributed over $[0, N_s T_f)$, Δ ($\Delta = T_c/N$ for $N \geq 1$) is the time resolution of the discrete-time equivalent channel impulse response (CIR) $h^{(k)}(t)$ obtained from the IEEE 802.15.3a standard UWB channel model [15].

As a realistic UWB channel model, the *discrete-time equivalent CIR* is generated as follows:

$$h^{(k)}(t) = \sum_{m \geq 0} \sum_{n \geq 0} \alpha_{n,m} \delta(t - T_m - \tau_{n,m}) \quad (3)$$

where $\alpha_{n,m}$ is the channel gain of nth ray in mth cluster and $\tau_{n,m}$ is the arrival time of nth ray relative to mth cluster's arrival time T_m. Here, the inter-cluster and inter-ray arrival times are independently exponentially distributed. $\alpha_{n,m} = p_{n,m}\beta_{n,m}$ where $p_{n,m}$ equiprobably takes on the values of ± 1 accounting for the random pulse inversion that occurs due to reflections and $\beta_{n,m}$ is a lognormal random variable where $20 \log_{10}(\beta_{n,m})$ is Gaussian with mean $\mu_{n,m}$ and variance σ^2. The power profile is double exponentially decaying, given by $\mathbf{E}\{\beta_{n,m}^2\} = \Omega_0 \exp(-T_m/\Gamma) \exp(-\tau_{n,m}/\gamma)$ ($\mathbf{E}$ denotes the expectation), where Ω_0 is the mean power of first ray of first cluster (i.e., $m = n = 0$), Γ and γ represent the power decay factors of the cluster and ray, respectively.

In the lth time bin $[\, l\Delta, (l+1)\Delta)$, one or more multipath components (MPCs) can arrive because of *cluster overlapping*, or no arrival at all (i.e., channel *sparseness*). The channel gains of all the arrived MPCs within that time bin are linearly combined to yield a composite channel gain $a_l^{(k)}$ in (2). It is to be noted that $a_l^{(k)}$ could be zero if there is no MPC in the lth time bin, and the channel delay spread (i.e., $T_{mds} = L\Delta$) is a variable depending on the type of IEEE channel models such as CM1 to CM4, where Ω_0 is set to meet $\sum_{l=0}^{L-1} \mathbf{E}\left\{ {a_l^{(k)}}^2 \right\} = 1$ for all k.

The signal received by the *desired* first user within one-symbol duration can be expressed by (assuming symbol '0' was transmitted by the first user)

$$\begin{aligned} r(t) = & \sqrt{\frac{E_1}{N_s}} \sum_{j=0}^{N_s-1} \sum_{l=0}^{L-1} a_l^{(1)} d_j^{(1)} b_0^{(1)} \\ & \cdot w_{rec}(t - jT_f - c_j^{(1)} T_c - l\Delta) \\ & + \sum_{k=2}^{K} \sqrt{\frac{E_k}{N_s}} \sum_{j=-\infty}^{\infty} \sum_{l=0}^{L-1} a_l^{(k)} d_j^{(k)} b_{\lfloor j/N_s \rfloor}^{(k)} \\ & \cdot w_{rec}(t - jT_f - c_j^{(k)} T_c - \tau^{(k)} - l\Delta) + n(t) \end{aligned} \quad (4)$$

where $w_{rec}(t)$ denotes the unit-energy received pulse that accounts for channel and antenna effects, which is assumed to be estimated (known) by the receiver, $\tau^{(1)} = 0$ is assumed for simplicity, and $n(t)$ is an additive white Gaussian noise (AWGN) with two-sided spectral density of $N_o/2$.

To exploit the two-dimensional diversity offered by UWB-IR signaling, the received signal is processed in parallel for both fingers $l = 0, 1, \ldots, L_p - 1$ ($L_p \leq L$) at *partial*-Rake receiver and frames $j = 0, 1, \ldots, N_s - 1$, as follows:

$$\begin{aligned} X_{l,j} &= \sqrt{\frac{N_s}{E_1}} \int_{jT_f}^{(j+1)T_f} r(t)\, d_j^{(1)} \\ &\quad \cdot w_{rec}(t - jT_f - c_j^{(1)} T_c - l\Delta)\, dt \\ &= a_l^{(1)} b_0^{(1)} + I_{l,j} + N_{l,j} \end{aligned} \quad (5)$$

where $I_{l,j}$ and $N_{l,j}$ represent the filtered multiuser interference (MUI) and noise of lth finger and jth frame, respectively. Here, $\{X_{l,j} \,|\, l = 0, \ldots, L_p - 1;\ j = 0, \ldots, N_s - 1\}$ form *sufficient statistics* for the following near-optimal decision, provided the filtered MUI is not any more Gaussian because of impulsive nature of collisions among user pulses. This *non-Gaussian* modeling of the MUI results in employing a nonlinear process at each finger, as implemented in the following section.

III. Near-Optimal and Suboptimal Receivers

First, it is noted that the filtered MUI $I_{l,j}$ is caused by any possible collisions with other user pulses, thereby exhibiting the nature of impulsive noise, which necessitates nonlinear processing to properly deal with occasional undue increases in the MUI across both fingers and frames. This is in contrast to conventional linear processing to mitigate the MUI by virtue of averaging over fingers and frames with linear weights. In determining a proper form of nonlinear processing, it is prerequisite to characterize the filtered MUI statistics that are modeled as *non-Gaussian* or *generalized* Gaussian distribution [11].

A. Filtered MUI statistics

The filtered MUI $I_{l,j}$ in (5), or equivalently $I_{l,j} = \sum_{k=2}^{K} I_{l,j}^{(k)}$ can be formulated as

$$\begin{aligned} I_{l,j}^{(k)} = \sqrt{\frac{E_k}{E_1}} \int_{jT_f}^{(j+1)T_f} d_j^{(1)} \Big[& d_{j'}^{(k)} b_{\lfloor j'/N_s \rfloor}^{(k)} \\ & \cdot \sum_{l_1} a_{l_1}^{(k)} w_{rec}(t - \tilde{\tau}^{(1)} - \theta_{j',j}^{(k)} - l_1\Delta) + d_{j'-1}^{(k)} b_{\lfloor j'-1/N_s \rfloor}^{(k)} \\ & \cdot \sum_{l_2} a_{l_2}^{(k)} w_{rec}(t + T_f - \tilde{\tau}^{(1)} - \theta_{j'-1,j}^{(k)} - l_2\Delta) \Big] \\ & \cdot w_{rec}(t - \tilde{\tau}^{(1)} - l\Delta)\, dt \end{aligned} \tag{6}$$

where the *desired* first user's reference time is $\tilde{\tau}^{(1)} \triangleq jT_f + c_j^{(1)} T_c$, assuming $\tau^{(1)} = 0$, and the kth user's reference time $\tilde{\tau}^{(k)} \triangleq \tau^{(k)} + j'T_f + c_{j'}^{(k)} T_c$ can be related to $\tilde{\tau}^{(1)}$ as

$$\tilde{\tau}^{(k)} = \tilde{\tau}^{(1)} + \theta_{j',j}^{(k)}$$

where $\theta_{j',j}^{(k)} = \left[c_{j'}^{(k)} - c_j^{(1)} \right] T_c + \delta^{(k)}$ and $\delta^{(k)} = \tau^{(k)}$ modulo T_f is uniformly distributed over $[0, T_f)$ for $\tau^{(k)} = j^{(k)} T_f + \delta^{(k)}$ and $j' = j - j^{(k)}$. Note that $l_i \in \{0, 1, \ldots, L-1\}$ $(i = 1, 2)$ can be found for any full or partial overlaps between the first user pulse and kth user current (j') and previous ($j'-1$) pulses, respectively. By defining $R_w(x) = \int_{-\infty}^{\infty} w_{rec}(t) w_{rec}(t-x)\, dt$, (6) is further simplified to

$$\begin{aligned} I_{l,j}^{(k)} = \sqrt{\frac{E_k}{E_1}}\, d_j^{(1)} \Big[& d_{j'}^{(k)} b_{\lfloor j'/N_s \rfloor}^{(k)} \\ & \cdot \sum_{l_1} a_{l_1}^{(k)} R_w\Big(\theta_{j',j}^{(k)} + (l_1 - l)\Delta \Big) + d_{j'-1}^{(k)} b_{\lfloor j'-1/N_s \rfloor}^{(k)} \\ & \cdot \sum_{l_2} a_{l_2}^{(k)} R_w\Big(\theta_{j'-1,j}^{(k)} - T_f + (l_2 - l)\Delta \Big) \Big]. \end{aligned} \tag{7}$$

To characterize the filtered MUI statistics as impulsive noise (i.e., non-Gaussian), this paper attempts to invoke the generalized Gaussian (GG) distribution and theoretically estimate a GG parameter (ν) by directly evaluating the second and fourth order moments of the MUI below.

In the following, the procedure of representing the MUI $I_{l,j}$ with its equivalent GG distribution $f_{I_{l,j}}(x)$ is presented. Modeling the MUI by the GG distribution is first proposed in [11] when the maximal-ratio combined (MRC) output is considered at *full*-Rake receiver, but here the GG distribution is used to fit the distribution of the MUI $I_{l,j}$ for each finger at *partial*-Rake receiver, following the approach in [14]. This GG distribution can be represented by [16]

$$f_{I_{l,j}}(x) = \frac{c_1(\nu)}{\sqrt{\sigma_l^2}} \exp\left(-c_2(\nu) \left| \frac{x}{\sqrt{\sigma_l^2}} \right|^{\nu} \right) \tag{8}$$

where $\sigma_l^2 = \mathbf{E}\{I_{l,j}^2\}$ is the variance of the GG distribution,

$$c_1(\nu) = \frac{\Gamma^{1/2}(3/\nu)}{(2/\nu)\Gamma^{3/2}(1/\nu)} \quad \text{and} \quad c_2(\nu) = \left[\frac{\Gamma(3/\nu)}{\Gamma(1/\nu)} \right]^{\nu/2}$$

for $\nu > 0$ and the Gamma function $\Gamma(x) = \int_0^{\infty} u^{x-1} e^{-u} du$. Here, the nth order moment of a GG variable X is given by [17]

$$\mathbf{E}\{X^n\} = \frac{\Gamma[(n+1)/\nu]}{\Gamma(1/\nu)} \left[\frac{\Gamma(1/\nu)}{\Gamma(3/\nu)}\, \sigma_l^2 \right]^{n/2} \tag{9}$$

for an even number n and $\mathbf{E}\{X^n\} = 0$ for an odd number n. Based on (9), the relation between the kurtosis ζ of X and ν can be obtained as [11]

$$\zeta = \frac{\mathbf{E}\{X^4\}}{\mathbf{E}^2\{X^2\}} - 3 = \frac{\Gamma(1/\nu)\Gamma(5/\nu)}{\Gamma^2(3/\nu)} - 3. \tag{10}$$

This means that by evaluating the second and fourth order moments of the MUI $I_{l,j}$, the kurtosis value ζ can be obtained, which can then be used to find the corresponding GG parameter ν. Once the parameter ν is determined, the GG distribution $f_{I_{l,j}}(x)$ that models the distribution of $I_{l,j}$ can be obtained, since it is only a function of ν and σ_l^2.

To validate the *non-Gaussian* modeling of the MUI via the GG distribution, we should be able to theoretically evaluate the second and fourth order moments of the MUI $I_{l,j}$, which allows to estimate the parameter ν. The following propositions are useful in evaluating the MUI statistics for the realistic UWB channel in (2) where the channel *sparseness* and *cluster overlapping* are accounted for [18].

Proposition 1: The second order moment or variance of the MUI $I_{l,j}$ is evaluated as

$$\begin{aligned} \sigma_l^2 &= \mathbf{E}\{I_{l,j}^2\} \\ &= \sum_{k=2}^{K} \left(\frac{E_k}{E_1} \right) \frac{1}{N_f} \sum_{n=-N_f}^{N_f-1} \sum_{m=0}^{N} \mathbf{E}\left\{ \left(a_{l-nN-m}^{(k)} \right)^2 \right\} \kappa_m \end{aligned} \tag{11}$$

where $N_f = T_f/T_c$ and $\kappa_m = \mathbf{E}\{R_w^2(\epsilon - m\Delta)\}$ with the expectation taken for the chip time-offset ϵ, uniformly distributed over $[0, T_c)$. Note that if $\Delta = T_c$ (i.e., $N = 1$), the above is simplified to

$$\sigma_l^2 = \mathbf{E}\{I_{l,j}^2\} = \sum_{k=2}^{K} \left(\frac{E_k}{E_1} \right) \left(\frac{2\kappa_0}{N_f} \right)$$

by the relation $\sum_{l=0}^{L-1} \mathbf{E}\left\{ {a_l^{(k)}}^2 \right\} = 1$ for all k.

Proof of proposition 1: see Appendix A.

Note that the filtered MUIs $\{I_{l,j}\}$ at each finger show the same variance across the frames ($j = 0, 1, \ldots, N_s - 1$), and they are assumed to be independent of each other because collision occurs independently from frame to frame, under the constraint of no IFI and random TH shift. However, $\{I_{l,j}\}$ in a given frame are *pair-wise* correlated across the fingers ($l = 0, 1, \ldots, L_p - 1$) because two adjacent fingers see the MUIs caused by partial collisions with the same user pulse, as long as the chip time-offset ϵ is not zero. In practice, $\mathbf{E}\{R_w(\epsilon) R_w(T_c - \epsilon)\}$ is almost negligible, since $R_w(\epsilon) \cong 0$ for $|\epsilon| \geq T_c/2$ when $w_{rec}(t)$ is the second order Gaussian monocycle. Hence, $\{I_{l,j}\}$ are assumed to be *weakly* uncorrelated but not independent of each other (i.e., non-Gaussian) across the fingers, whereas they are assumed to be independent across the frames.

Proposition 2: The fourth order moment of the MUI $I_{l,j}$ is

evaluated as

$$\begin{aligned}\mathbf{E}\{I_{l,j}^4\} = &\sum_{k=2}^{K}\left(\frac{E_k}{E_1}\right)^2\frac{1}{N_f}\\ &\cdot\sum_{n=-N_f}^{N_f-1}\Bigg[\sum_{m=0}^{N}\mathbf{E}\Big\{\Big(a_{l-nN-m}^{(k)}\Big)^4\Big\}\varphi_m\\ &+6\sum_{m=0}^{N-1}\sum_{m'=m+1}^{N}\mathbf{E}\Big\{\Big(a_{l-nN-m}^{(k)}\Big)^2\Big\}\\ &\cdot\mathbf{E}\Big\{\Big(a_{l-nN-m'}^{(k)}\Big)^2\Big\}\rho_{m,m'}\Bigg]\\ &+6\sum_{k=2}^{K-1}\sum_{k'=k+1}^{K}\left(\frac{E_k}{E_1}\right)\left(\frac{E_{k'}}{E_1}\right)\\ &\cdot\left[\frac{1}{N_f}\sum_{n=-N_f}^{N_f-1}\sum_{m=0}^{N}\mathbf{E}\Big\{\Big(a_{l-nN-m}^{(k)}\Big)^2\Big\}\kappa_m\right]^2 \quad (12)\end{aligned}$$

where $\varphi_m = \mathbf{E}\{R_w^4(\epsilon - m\Delta)\}$ and $\rho_{m,m'} = \mathbf{E}\{R_w^2(\epsilon - m\Delta)R_w^2(\epsilon - m'\Delta)\}$. Note that if $\Delta = T_c$ (i.e., $N = 1$), the above is simplified to

$$\begin{aligned}\mathbf{E}\{I_{l,j}^4\} = &\sum_{k=2}^{K}\left(\frac{E_k}{E_1}\right)^2\Bigg[\left(\frac{2\varphi_0}{N_f}\right)\sum_{n=0}^{L-1}\mathbf{E}\Big\{a_n^{(k)\,4}\Big\}\\ &+\left(\frac{6\rho_{0,1}}{N_f}\right)\sum_{n=1}^{L-1}\mathbf{E}\Big\{a_n^{(k)\,2}\Big\}\mathbf{E}\Big\{a_{n-1}^{(k)\,2}\Big\}\Bigg]\\ &+6\sum_{k=2}^{K-1}\sum_{k'=k+1}^{K}\left(\frac{E_k}{E_1}\right)\left(\frac{E_{k'}}{E_1}\right)\left(\frac{2\kappa_0}{N_f}\right)^2\end{aligned}$$

Proof of proposition 2: see Appendix B.

To find $\mathbf{E}\{I_{l,j}^4\}$ in *closed-form*, the second and fourth order moments of the channel gains $\{a_n^{(k)}\}$ should be evaluated, considering a realistic, standard UWB channel with lognormal channel gain distribution and double independent Poisson arrival distribution of cluster and ray [15].

Proposition 3: The second order moment of the composite channel gain $a_n^{(k)}$ is evaluated as

$$\mathbf{E}\Big\{a_n^{(k)\,2}\Big\} = \begin{cases}\Omega_0, & \text{for } n = 0\\ \Omega_0 P_c\exp\left[-\dfrac{n\Delta}{\Gamma}\right] + \Omega_0 P_r\exp\left[-\dfrac{n\Delta}{\gamma}\right]\\ \quad+\Omega_0 P_c P_r\dfrac{\eta^2(1-\eta^{n-1})}{1-\eta}\\ \quad\cdot\exp\left[-\dfrac{(n+1)\Delta}{\gamma}+\dfrac{\Delta}{\Gamma}\right], & \text{for } n \geq 1\end{cases} \quad (13)$$

where $P_c = \Lambda\Delta$ and $P_r = \lambda\Delta$ (Λ and λ denote the cluster and ray arrival rates, respectively), and $\eta = \exp\left(\frac{\Delta}{\gamma} - \frac{\Delta}{\Gamma}\right)$. Also, by defining $\bar{E}_c \triangleq \sum_{n=0}^{L-1}\mathbf{E}\Big\{a_n^{(k)\,2}\Big\}$, the mean power of first ray of first cluster Ω_0 can be theoretically determined as

$$\Omega_0 = \frac{1}{\bar{E}_0} \triangleq \frac{1}{\bar{E}_c|_{\Omega_0=1}} \quad (14)$$

so as to make $\bar{E}_c = 1$ (normalized).

Proof of proposition 3: refer to [18, eqs. (18) and (19)].

Proposition 4: The fourth order moment of the composite channel gain $a_n^{(k)}$ is evaluated as

$$\begin{aligned}\mathbf{E}\Big\{a_n^{(k)\,4}\Big\} = &\sum_{q=0}^{n}\Omega_0^2 P_q^{(n)}\exp\left[-\frac{2q\Delta}{\Gamma}\right]\\ &\cdot\exp\left[-\frac{2(n-q)\Delta}{\gamma}\right]\exp\left[\frac{\sigma^2}{\xi^2}\right]\\ &+6\sum_{q=0}^{n-1}\sum_{j=q+1}^{n}\Omega_0^2 P_q^{(n)}P_j^{(n)}\\ &\cdot\exp\left[-\frac{(q+j)\Delta}{\Gamma}\right]\exp\left[-\frac{(2n-q-j)\Delta}{\gamma}\right] \quad (15)\end{aligned}$$

where $\xi = 10/\ln 10$, and the probability that qth ($q = 0, 1, \ldots, n$) time bin has a MPC (either ray or cluster) contribution to nth ($n \geq 1$) time bin $[nT_c, (n+1)T_c)$, denoted by $P_q^{(n)}$, can be calculated in three cases: [18]

$$P_q^{(n)} = \begin{cases}P_r, & q = 0\\ P_c\cdot P_r, & 1 \leq q \leq n-1\\ P_c, & q = n\end{cases} \quad (16)$$

with $P_q^{(n)} = 1$ for $q = n = 0$.

Proof of proposition 4: see Appendix C.

Now, combining the above *propositions 1-4* provides an estimate of the GG parameter ν in (10), which then yields the GG distribution $f_{I_{l,j}}(x)$ in (8).

Fig. 1 shows how the filtered MUI $I_{l,j}$ closely follows the GG distribution obtained theoretically using the parameter ν or equivalently the second and fourth order moments.

B. Near-optimal nonlinear processing

Note that the GG distribution of $\{I_{l,j} \mid j = 0, 1, \ldots, N_s - 1\}$ is assumed to be independent across the frames, in which case a nonlinear process to suppress an excessive MUI at a fixed lth finger can be implemented, following the approach in [14].

Forming the N_s-dimensional observation space across the frames, an observation vector $\mathbf{X}_l \triangleq (X_{l,0}, X_{l,1}, \ldots, X_{l,N_s-1})$, where $X_{l,j} = a_l^{(1)}b_0^{(1)} + I_{l,j} + N_{l,j}$ in (5), is applied to the nonlinear process that performs the maximum-likelihood (ML) decision for H_1 ($b_0^{(1)} = 1$) if

$$\frac{f_{\mathbf{X}_l}(\mathbf{x}_l \mid a_l^{(1)}, b_0^{(1)} = 1)}{f_{\mathbf{X}_l}(\mathbf{x}_l \mid a_l^{(1)}, b_0^{(1)} = -1)} > 1 \quad (17)$$

and otherwise for H_0 ($b_0^{(1)} = -1$). If the excessive MUI becomes dominant and the noise term $N_{l,j}$ can be ignored, the ML decision for H_1 can be rewritten as

$$\frac{\prod_{j=0}^{N_s-1} f_{I_{l,j}}(x_{l,j} - a_l^{(1)} \mid a_l^{(1)}, b_0^{(1)} = 1)}{\prod_{j=0}^{N_s-1} f_{I_{l,j}}(x_{l,j} + a_l^{(1)} \mid a_l^{(1)}, b_0^{(1)} = -1)} > 1. \quad (18)$$

After a few mathematical steps [11], it follows that

$$\sum_{j=0}^{N_s-1} h_l(x_{l,j}) > 0 \quad \Rightarrow \quad H_1 \quad (19)$$

where the *nonlinear function* $h_l(x)$ employed at the lth finger is defined by

$$h_l(x) = \left|x + a_l^{(1)}\right|^\nu - \left|x - a_l^{(1)}\right|^\nu \quad (20)$$

with $a_l^{(1)}$ being estimated for diversity combining.

Note that, if the decision statistics $\mathbf{X}_j \triangleq (X_{0,j}, X_{1,j}, \ldots, X_{L_p-1,j})$ can also be assumed to be independent,[1] the ML decision in (19) that exploits two-dimensional diversity (i.e., multipath and repetition diversity) can easily be generalized to

$$\sum_{l=0}^{L_p-1} \sum_{j=0}^{N_s-1} h_l(x_{l,j}) > 0 \quad \Rightarrow \quad H_1. \tag{21}$$

It should be noted that the *generalized* ML decision rule in (21) is not optimal because the MUI is not any more Gaussian, which may be classified as *near-optimal*. In fact, if the MUI becomes Gaussian (i.e., $\nu = 2$), the ML decision results in classical MRC receiver as

$$\sum_{l=0}^{L_p-1} a_l^{(1)} \left(\sum_{j=0}^{N_s-1} x_{l,j} \right) > 0 \quad \Rightarrow \quad H_1. \tag{22}$$

C. Suboptimal nonlinear processing

Following the approach in [11], a suboptimal receiver is implemented that applies the MRC output across the fingers in each frame, to a nonlinear process and that performs the ML decision based on the GG distribution of the MRC outputs.[2]

Let define the MRC output in the jth frame as

$$Y_j = \sum_{l=0}^{L_p-1} a_l^{(1)} X_{l,j} = S b_0^{(1)} + \tilde{I}_j + \tilde{N}_j, \quad j = 0, 1, \ldots, N_s - 1, \tag{23}$$

where $S = \sum_{l=0}^{L_p-1} {a_l^{(1)}}^2$, $\tilde{I}_j = \sum_{l=0}^{L_p-1} a_l^{(1)} I_{l,j}$, $\tilde{N}_j = \sum_{l=0}^{L_p-1} a_l^{(1)} N_{l,j}$, and an observation vector $\mathbf{Y} \triangleq (Y_0, Y_1, \ldots, Y_{N_s-1})$ is applied to the nonlinear process. Then, if the combined MUI becomes dominant and the noise term $\tilde{N}_j$ can be ignored, the ML decision for H_1 is made based on

$$\frac{f_{\mathbf{Y}}(\mathbf{y}_j \mid a_l^{(1)}, b_0^{(1)} = 1)}{f_{\mathbf{Y}}(\mathbf{y}_j \mid a_l^{(1)}, b_0^{(1)} = -1)} = \frac{\prod_{j=0}^{N_s-1} f_{\tilde{I}_j}(y_j - S \mid a_l^{(1)}, b_0^{(1)} = 1)}{\prod_{j=0}^{N_s-1} f_{\tilde{I}_j}(y_j + S \mid a_l^{(1)}, b_0^{(1)} = -1)} > 1$$
$$\sum_{j=0}^{N_s-1} h(y_j) > 0 \quad \Rightarrow \quad H_1 \tag{24}$$

where the nonlinear function $h(y)$ is found in (20) with $a_l^{(1)}$ replaced by S and corresponding ν.

Similarly, the GG parameter ν is determined by directly evaluating the second and fourth order moments of the combined MUI $\tilde{I}_j$ after MRC as follows.

Proposition 5 : Assuming $\Delta = T_c$ (i.e., $N = 1$) for the MRC output, the second and fourth order moments of the combined MUI $\tilde{I}_j$ are evaluated as

$$\mathbf{E}\{\tilde{I}_j^2\} \cong \sum_{l=0}^{L_p-1} \mathbf{E}\left\{ {a_l^{(1)}}^2 \right\} \sum_{k=2}^{K} \left(\frac{E_k}{E_1} \right) \left(\frac{2\kappa_0}{N_f} \right) \tag{25}$$

$$\begin{aligned} \mathbf{E}\{\tilde{I}_j^4\} \cong & \sum_{l=0}^{L_p-1} \mathbf{E}\left\{ {a_l^{(1)}}^4 \right\} \left\{ \sum_{k=2}^{K} \left(\frac{E_k}{E_1} \right)^2 \left[\left(\frac{2\varphi_0}{N_f} \right) \sum_{n=0}^{L-1} \right. \right. \\ & \cdot \mathbf{E}\left\{ {a_n^{(k)}}^4 \right\} + \left(\frac{6\rho_{0,1}}{N_f} \right) \sum_{n=1}^{L-1} \mathbf{E}\left\{ {a_n^{(k)}}^2 \right\} \mathbf{E}\left\{ {a_{n-1}^{(k)}}^2 \right\} \left. \right] \\ & + 6 \sum_{k=2}^{K-1} \sum_{k'=k+1}^{K} \left(\frac{E_k}{E_1} \right) \left(\frac{E_{k'}}{E_1} \right) \left(\frac{2\kappa_0}{N_f} \right)^2 \left. \right\} \\ & + 6 \sum_{l=0}^{L_p-2} \sum_{l'=l+1}^{L_p-1} \mathbf{E}\left\{ {a_l^{(1)}}^2 \right\} \mathbf{E}\left\{ {a_{l'}^{(1)}}^2 \right\} \left\{ \sum_{k=2}^{K} \right. \\ & \cdot \left(\frac{E_k}{E_1} \right)^2 \left(\frac{2\varphi_0}{N_f} \right) \sum_{n=1}^{L-1} \mathbf{E}\left\{ {a_n^{(k)}}^2 \right\} \mathbf{E}\left\{ \left(a_{n+l'-l}^{(k)} \right)^2 \right\} \\ & + 2 \sum_{k=2}^{K-1} \sum_{k'=k+1}^{K} \left(\frac{E_k}{E_1} \right) \left(\frac{E_{k'}}{E_1} \right) \left(\frac{2\kappa_0}{N_f} \right)^2 \left. \right\}. \end{aligned} \tag{26}$$

Proof of proposition 5 : see Appendix D.

Thus, combining the above *propositions 3-5* provides an estimate of the GG parameter ν in (10), which then yields the GG distribution $f_{\tilde{I}_j}(y)$ in (8) with $\sigma_l^2 = \mathbf{E}\{\tilde{I}_j^2\}$.

Fig. 2 demonstrates how the combined MUI $\tilde{I}_j$ closely follows the GG distribution obtained theoretically using the parameter ν or equivalently the second and fourth order moments.

In the following section, the three receivers, such as near-optimal receiver, suboptimal receiver, and classical MRC receiver are compared in terms of the *channel-averaged* bit-error rate (BER) when both the MUI and AWGN are present.

IV. *Channel-Averaged* BER

Combining (20) and (21), the decision variable after near-optimal nonlinear processing becomes

$$\begin{aligned} \Phi &\triangleq \sum_{l=0}^{L_p-1} \sum_{j=0}^{N_s-1} h_l\left(\Xi_{l,j} + a_l^{(1)} \right) \\ &= \sum_{l=0}^{L_p-1} \sum_{j=0}^{N_s-1} \left| \Xi_{l,j} + 2a_l^{(1)} \right|^\nu - \left| \Xi_{l,j} \right|^\nu \end{aligned} \tag{27}$$

where $X_{l,j} = \Xi_{l,j} + a_l^{(1)}$ with $\Xi_{l,j} = I_{l,j} + N_{l,j}$, assuming $b_0^{(1)} = 1$ without loss of generality. Note that, the composite GG variable $\Xi_{l,j}$ can be described by the GG distribution in (8) with $\sigma_l^2 = \mathbf{E}\{\Xi_{l,j}^2\} = \mathbf{E}\{I_{l,j}^2\} + \mathbf{E}\{N_{l,j}^2\}$ and $\mathbf{E}\{\Xi_{l,j}^4\} = \mathbf{E}\{I_{l,j}^4\} + 6\,\mathbf{E}\{I_{l,j}^2\}\,\mathbf{E}\{N_{l,j}^2\} + \mathbf{E}\{N_{l,j}^4\}$, where $\mathbf{E}\{N_{l,j}^2\} = N_s(2E_1/N_o)^{-1}$ and $\mathbf{E}\{N_{l,j}^4\} = 3\,\mathbf{E}^2\{N_{l,j}^2\}$. The corresponding GG parameter ν in (27) can be estimated by (10) using the above two moments of the composite GG variable $\Xi_{l,j}$.

Similarly, the decision variable in (24) after suboptimal nonlinear processing is defined as

$$\tilde{\Phi} \triangleq \sum_{j=0}^{N_s-1} h\left(\tilde{\Xi}_j + S \right) = \sum_{j=0}^{N_s-1} \left| \tilde{\Xi}_j + 2S \right|^\nu - \left| \tilde{\Xi}_j \right|^\nu \tag{28}$$

[1] If the GG parameter ν approaches 2 (i.e., the MUI becomes Gaussian), they can be assumed to be *weakly* independent of each other as $\{I_{l,j}\}$ are *weakly* uncorrelated across the fingers.

[2] For validation of modeling the MRC output by the GG distribution, refer to Fig. 2 in [11].

where $Y_j = \tilde{\Xi}_j + S$ with $\tilde{\Xi}_j = \tilde{I}_j + \tilde{N}_j$, assuming $b_0^{(1)} = 1$ without loss of generality. Note that, the composite GG variable $\tilde{\Xi}_j$ can also be described by the corresponding GG distribution with $\sigma_l^2 = \mathbf{E}\{\tilde{\Xi}_j^2\} = \mathbf{E}\{\tilde{I}_j^2\} + \mathbf{E}\{\tilde{N}_j^2\}$ and $\mathbf{E}\{\tilde{\Xi}_j^4\} = \mathbf{E}\{\tilde{I}_j^4\} + 6\,\mathbf{E}\{\tilde{I}_j^2\}\,\mathbf{E}\{\tilde{N}_j^2\} + \mathbf{E}\{\tilde{N}_j^4\}$, where $\mathbf{E}\{\tilde{N}_j^2\} = \sum_{l=0}^{L_p-1} \mathbf{E}\left\{a_l^{(1)^2}\right\}\mathbf{E}\{N_{l,j}^2\}$ and

$$\mathbf{E}\{\tilde{N}_j^4\} = \sum_{l=0}^{L_p-1} \mathbf{E}\left\{a_l^{(1)^4}\right\}\mathbf{E}\{N_{l,j}^4\} + 6\sum_{l=0}^{L_p-2}\sum_{l'=l+1}^{L_p-1} \mathbf{E}\left\{a_l^{(1)^2}\right\} \cdot \mathbf{E}\left\{a_{l'}^{(1)^2}\right\}\mathbf{E}\{N_{l,j}^2\}\mathbf{E}\{N_{l',j}^2\}.$$

Hence, the GG parameter ν in (28) can similarly be determined using the above two moments of the composite GG variable $\tilde{\Xi}_j$.

Finally, the decision variable for classical MRC receiver is obtained simply by letting $h(y) = y$ in (28), since (22) is equivalent to (24) with $h(y) = y$, which is

$$\hat{\Phi} = \sum_{j=0}^{N_s-1} \tilde{\Xi}_j + S, \tag{29}$$

assuming $b_0^{(1)} = 1$ without loss of generality.

Note that, if the decision variables in (27), (28) and (29) are compared to zero threshold and do not exceed it, it leads to the BER when *channel-averaged* through the simulations below.

V. Results

To validate the *non-Gaussian* distribution of the MUI, and for analytical and simulation purposes, the UWB standard IEEE 802.15.3a channel models have been used [15]. Without loss of generality, the results are presented only for the CM1, where the channel *sparseness* and *cluster overlapping* are accounted for, which represents a line-of-sight (LOS) channel measurement with a transceiver separation of 0-4m. The continuous-time channel impulse response (CIR) is sampled at 6GHz so that the discrete-time CIR is obtained with $N = 1$, and the channel delay spread T_{mds} is about 33ns, equal to about $200T_c$ ($L = 200$) for the CM1. The received pulse is assumed to be the second order derivative of Gaussian pulse with pulse width of 0.167ns (equal to the chip time T_c). The frame time $T_f = T_{mds} + N_h T_c = 250T_c$ is set to avoid the IFI and is fixed for all users.

Figs. 1 and 2 show the probability density function (*pdf*) of the filtered MUI $I_{l,j}$ in (5) and the MUI $\tilde{I}_j$ in (23) after MRC, respectively. Here, the *partial*-Rake with $L_p = 10$ taps has been used, the number of users is $K = 5$ and the number of frames is $N_s = 8$. Fig. 1 compares the *pdf* of the actual MUI (i.e., obtained from simulation) versus the estimated MUI, obtained from the adoption of different MUI models, such as Gaussian ($\nu = 2$), Laplace ($\nu = 1$), Gaussian mixture (GM)[3] and GG distributions. Especially, the GG model well approximates the non-Gaussian distribution of the actual MUI,

[3]Here, the GM model has used the statistics estimation approach proposed in Section III-B of [19].

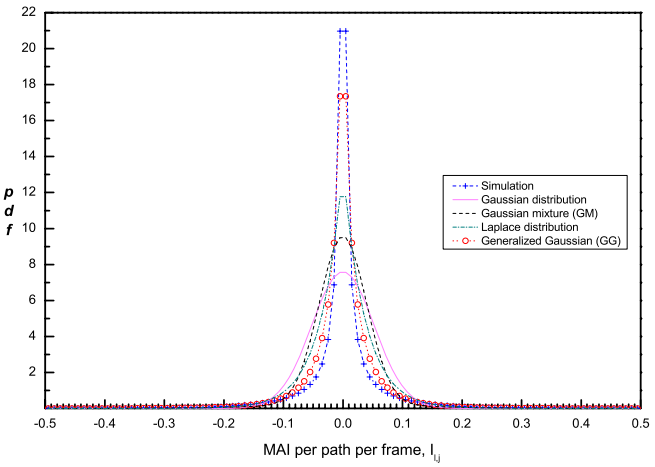

Fig. 1. *pdf* of the actual MUI versus the estimated MUI from different MUI models, such as Gaussian, Laplace, GM and GG, when $K = 5$ and $N_s = 8$, assuming the near-optimal (NO) receiver with *partial*-Rake of $L_p = 10$ taps.

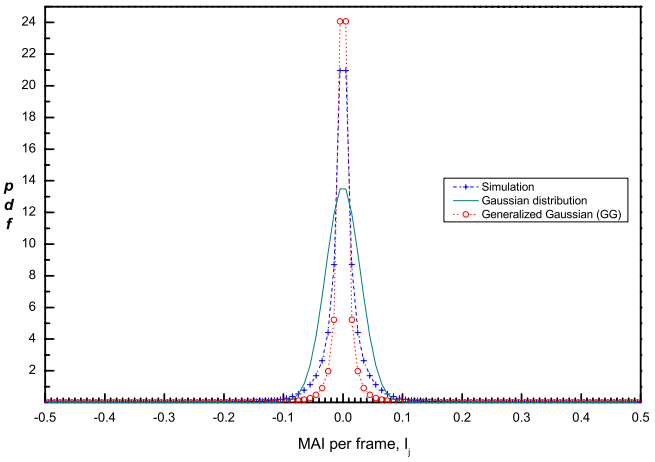

Fig. 2. *pdf* of the actual MUI versus the estimated MUI from GG model when $K = 5$ and $N_s = 8$, assuming the suboptimal (SO) receiver with *partial*-Rake of $L_p = 10$ taps.

where the GG parameter ν in (8) has been computed analytically through the evaluation of the corresponding second and fourth order moments in *propositions 1-5*.

For near-optimal (NO) and suboptimal (SO) receivers, the non-Gaussian nature of MUI statistics becomes apparent in Fig. 3 which shows the GG parameter ν as a function of L_p, relative to Gaussian distribution with $\nu = 2$. Here, the MUI statistics associated with NO receiver do not depend on the number of taps L_p at *partial*-Rake, whereas the MUI statistics of SO receiver change with L_p. In particular, the non-Gaussian nature is diminished as L_p increases because of the energy capture rapidly reaching the peak value (normalized to one), which makes the GG parameter ν increase. As expected, ν also increases with the number of users K, but it should be noted that *the non-Gaussian nature of MUI statistics persists even for relatively large* $K = 30$. Fig. 4 compares the GG parameter ν for varying N (time resolution of discrete-time CIR) where $\Delta = T_c/N$ in (2) for $N \geq 1$. It is shown that the GG parameter with $N = 1$ is within acceptable range, and it converges fastly when near at $N = 5$ (i.e., 5 times oversampling or sampling at 30GHz).

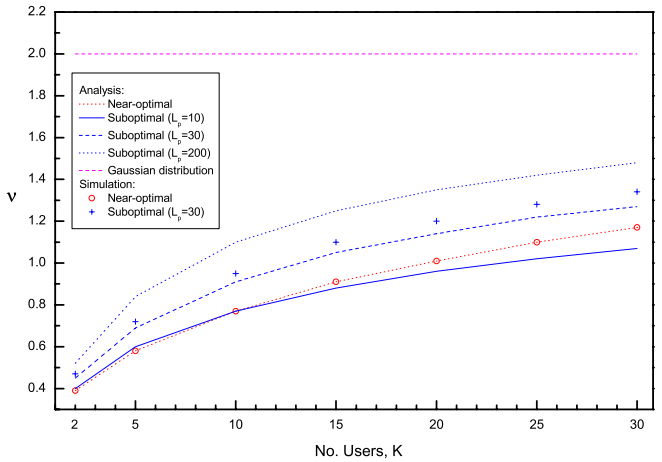

Fig. 3. GG parameter ν versus K when $N_s = 8$, assuming the NO and SO receivers with *partial*-Rake of $L_p = 10, 30, 200$ taps.

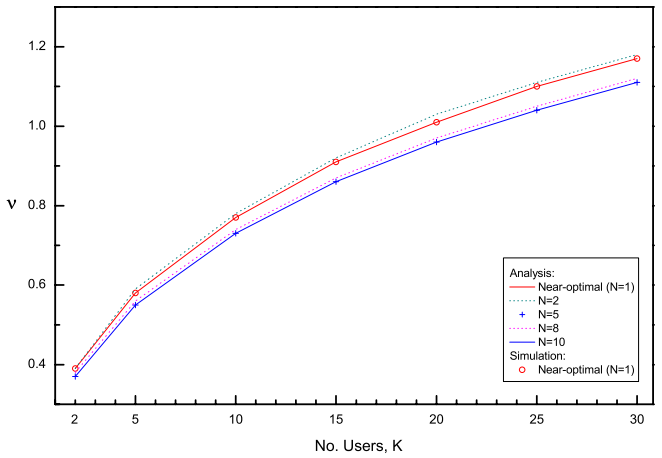

Fig. 4. GG parameter ν versus K for varying N (time resolution of discrete-time CIR) when $N_s = 8$, assuming the NO receiver with *partial*-Rake of $L_p = 10$ taps.

Next, the performance improvement offered by NO and SO receivers is illustrated in Figs. 5-7, as the number of frames per symbol N_s reduces from 8, 4 down to 2. Especially, the *repetition diversity* that arises because of the repeated pulse transmission per symbol can clearly be observed for varying N_s here. First, the performance improvement by the NO receiver over classical MRC is shown to be significant for the range of $K = 2$ to 10, which is typical in indoor UWB communications. Second, a proper value of N_s needs to be determined considering the required data rate, as the data rate decreases with increased N_s but the diversity gain above increases with N_s. Third, the diversity gain by the SO receiver is not that significant because the non-Gaussian nature of MUI statistics is diminished after MRC, while it appears prominent across fingers before MRC. Note that, the GG parameter ν used for nonlinear processing in (20) has been predetermined analytically from the MUI statistics found in *propositions 1-5*, considering the GG distribution.

Fig. 8 compares the BER of the NO receiver (based on GG model) versus the GM receiver in [19], as well as the hybrid of above, i.e., the NO receiver that employs the channel estimation approach (based on GM model) proposed

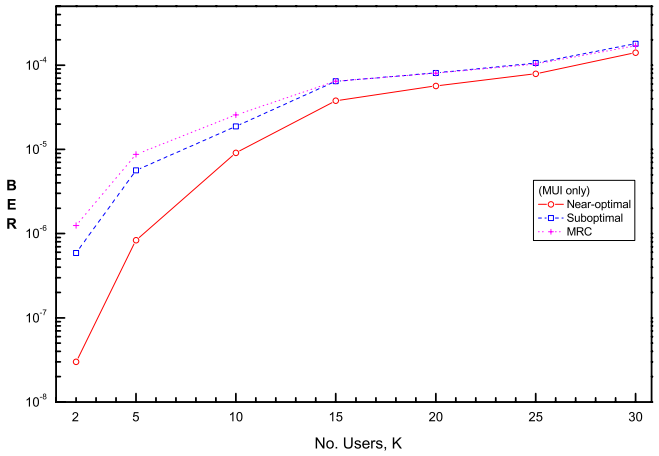

Fig. 5. *Channel-averaged* BER versus K when $N_s = 8$ and the MUI only exists, assuming the NO, SO, and MRC receivers with *partial*-Rake of $L_p = 10$ taps.

in Section III-C of [19]. To achieve the channel estimation, the NO receiver can simply adopt the training based approach proposed in [20] for which the preamble of length N_p bits precedes the data packet. First, the GM receiver performs better than the NO receiver when K is relatively large, but it performs worse as K decreases, because the GG model fits well the non-Gaussian MUI in Fig. 1 when $K = 5$. Second, the training based NO receiver with $N_p = 30$ provides a satisfactory BER compared to that of ideal NO receiver with perfect channel information. Third, the hybrid of NO/GM receiver performs quite well even with shorter preamble of $N_p = 10$ bits, which well exploits the advantages of NO and GM receivers.

To look into the effects of the IFI and noise on the diversity gain here, Fig. 9 shows the BER performance versus K in the presence of the IFI when $T_f = 150T_c < T_{mds} + N_hT_c = 250T_c$ and $N_s = 4$. Here, the effective received SNR for the *partial*-Rake was set to about 25dB, in which case the gain offered by the NO receiver is insignificant. This is because the non-Gaussian MUI is overwhelmed with the Gaussian noise when K is small, but as K increases (i.e., the MUI becomes dominant), the diversity gain reduces as shown in Fig. 6. It is interesting to see that the presence of the IFI necessitates using the NO receiver, since the MUI is relatively growing due to the IFI, which in turn somehow increases the diversity gain against MUI. Hence, if higher data rates are required and the IFI results, an optimal receiver needs to be designed by carefully considering the non-Gaussian nature of MUI statistics.

VI. Conclusion

Near-optimal and suboptimal receivers have been realized for UWB-IR systems by inserting nonlinear processing before MRC and after MRC in each frame, respectively, for which the MUI statistics were formulated. In particular, the *generalized* Gaussian modeling of the MUI was shown to be effective in deriving an order of such nonlinear processing, depending only on the second and fourth order moments. These MUI statistics have been analytically evaluated for realistic UWB channels that exhibit *sparseness* and *cluster overlapping*. The order of nonlinear processing, namely the GG parameter ν

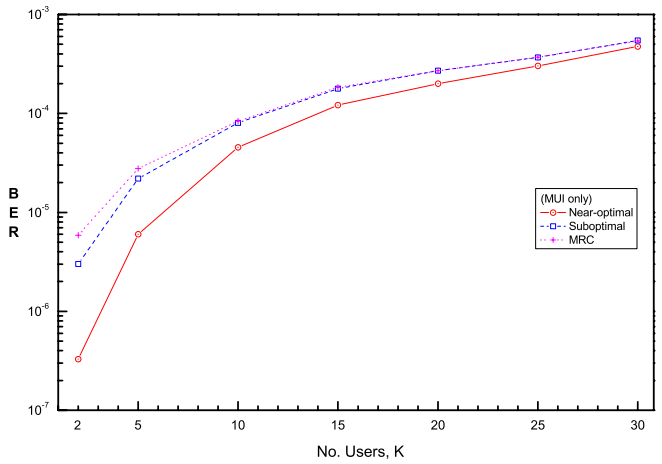

Fig. 6. *Channel-averaged* BER versus K when $N_s = 4$ and the MUI only exists, assuming the NO, SO, and MRC receivers with *partial*-Rake of $L_p = 10$ taps.

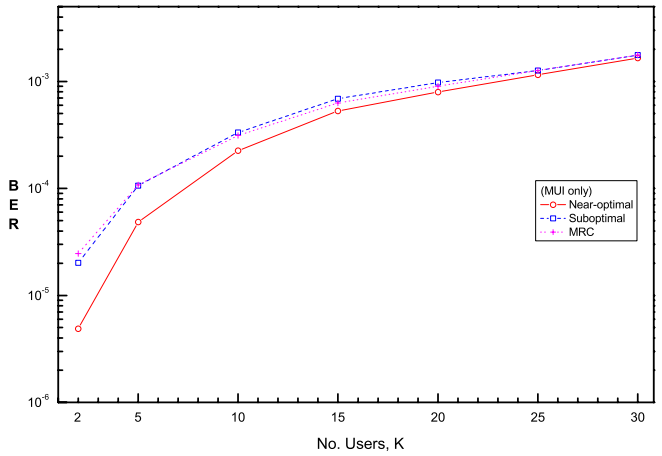

Fig. 7. *Channel-averaged* BER versus K when $N_s = 2$ and the MUI only exists, assuming the NO, SO, and MRC receivers with *partial*-Rake of $L_p = 10$ taps.

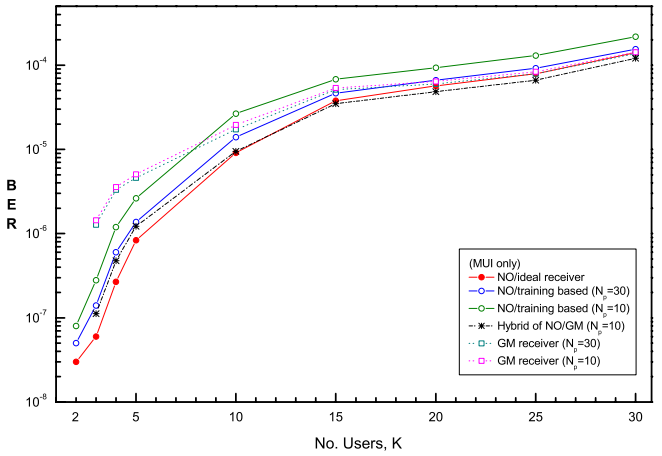

Fig. 8. *Channel-averaged* BER versus K when $N_s = 8$ and the MUI only exists, assuming the NO/ideal, NO/training based, GM, and hybrid of NO/GM receivers with *partial*-Rake of $L_p = 10$ taps.

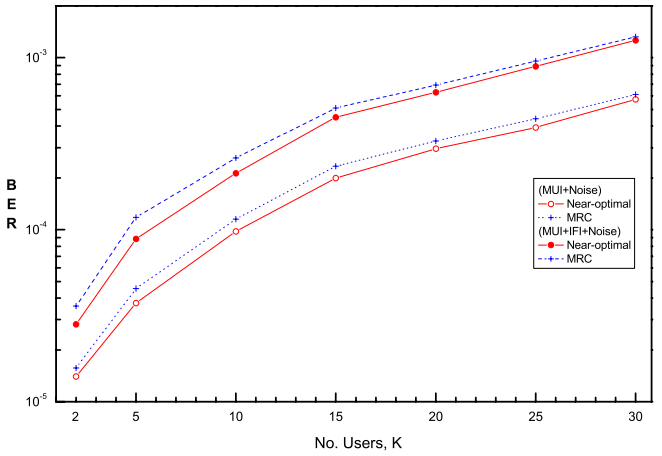

Fig. 9. *Channel-averaged* BER versus K when $N_s = 4$, the IFI and noise exist, assuming the NO and MRC receivers with *partial*-Rake of $L_p = 10$ taps.

was determined analytically for the assumed UWB channels, which reveals that the non-Gaussian nature of the MUI still exists for relatively large $K = 30$. This founding is in contrast to the previous observation that the MUI statistics approach Gaussian as K increases. From the BER analysis, it was observed that the diversity gain against MUI increases as the number of frames per symbol increases, as anticipated, but it decreases as K increases. Finally, as the data rate increases, the IFI would not be ignored because the channel delay spread appears longer in indoor wireless channels, in which case the non-Gaussian MUI will largely affect an optimal transceiver design in multiuser environment.

Appendix A
Proof of Proposition 1:

From (7) the second order moment σ_l^2 can be formulated as

$$\sigma_l^2 = \mathbf{E}\{I_{l,j}^2\} = \sum_{k=2}^{K}\left(\frac{E_k}{E_1}\right)\left[\sum_{l_1}\mathbf{E}\left\{{a_{l_1}^{(k)}}^2\right\}\mathbf{E}\left\{R_w^2\left(\theta_{j',j}^{(k)} + (l_1 - l)\Delta\right)\right\}\right.$$
$$\left. + \sum_{l_2}\mathbf{E}\left\{{a_{l_2}^{(k)}}^2\right\}\mathbf{E}\left\{R_w^2\left(\theta_{j'-1,j}^{(k)} - T_f + (l_2 - l)\Delta\right)\right\}\right] \quad (30)$$

where the cross-terms disappear since the MUI is zero-mean, uncorrelated across the users (index k), so are the channel coefficients across the MPCs (indexes l_i, $i = 1, 2$), and also due to the pseudorandom sequence.

Since the relative delay between desired and kth users $\theta_{j',j}^{(k)} = \left[c_{j'}^{(k)} - c_j^{(1)}\right]T_c + \delta^{(k)}$, and $\delta^{(k)} = \tau^{(k)}$ modulo T_f is uniformly distributed over $[0, T_f)$, σ_l^2 with fixed $c_j^{(1)}$ can be evaluated as

$$\sigma_l^2 = \sum_{k=2}^{K}\left(\frac{E_k}{E_1}\right)$$
$$\cdot\left[\sum_{l_1}\mathbf{E}\left\{{a_{l_1}^{(k)}}^2\right\}\frac{1}{T_f}\int_{-c_j^{(1)}T_c}^{T_f} R_w^2[x + (l_1 - l)\Delta]\,dx\right.$$
$$\left. + \sum_{l_2}\mathbf{E}\left\{{a_{l_2}^{(k)}}^2\right\}\frac{1}{T_f}\int_{-T_f}^{-c_j^{(1)}T_c} R_w^2[x + (l_2 - l)\Delta]\,dx\right]. \quad (31)$$

In the above, the average has been taken with respect to two

independent, identically distributed random variables $c_{j'}^{(k)}$ and $c_{j'-1}^{(k)}$, along with $R_w(x)=0$ for $|x|>T_c$ and the constraint of no IFI, namely $T_f \geq (L+N_h^{(k)})\,T_c$ for all k, by which the upper and lower integral limits can be set to $\pm T_f$ for simplicity. Hence, σ_l^2 is independent of a specific value $c_j^{(1)}$ and is simplified to

$$\sigma_l^2 = \sum_{k=2}^{K}\left(\frac{E_k}{E_1}\right)\sum_{l_1}\mathbf{E}\Big\{a_{l_1}^{(k)\,2}\Big\}\,\frac{1}{T_f}\int_{-T_f}^{T_f} R_w^2[x+(l_1-l)\Delta]\,dx. \tag{32}$$

Now, the index l_1 can be chosen to have non-zero correlation values for $R_w(x)$, where

$$\sigma_l^2 = \sum_{k=2}^{K}\left(\frac{E_k}{E_1}\right)\frac{1}{N_f}\sum_{n=-N_f}^{N_f-1}\frac{1}{T_c}\int_0^{T_c}\sum_{l_1}\mathbf{E}\Big\{a_{l_1}^{(k)\,2}\Big\} \cdot R_w^2[\epsilon+(l_1-l)\Delta+nT_c]\,d\epsilon, \tag{33}$$

and the selection of $l_1 = l-nN-m$, $m=0,1,\ldots,N$ produces non-zero correlations as

$$\sigma_l^2 = \sum_{k=2}^{K}\left(\frac{E_k}{E_1}\right)\frac{1}{N_f}\sum_{n=-N_f}^{N_f-1}\frac{1}{T_c} \cdot\int_0^{T_c}\left[\sum_{m=0}^{N}\mathbf{E}\Big\{\Big(a_{l-nN-m}^{(k)}\Big)^2\Big\}R_w^2(\epsilon-m\Delta)\right]d\epsilon. \tag{34}$$

By defining $\kappa_m = \mathbf{E}\{R_w^2(\epsilon-m\Delta)\}$ for the chip time-offset ϵ, uniformly distributed over $[0,T_c)$, σ_l^2 in (34) reduces to (11).

APPENDIX B
PROOF OF PROPOSITION 2:

The fourth order moment $\mathbf{E}\{I_{l,j}^4\}$ can be expressed by

$$\mathbf{E}\{I_{l,j}^4\} = \sum_{k=2}^{K}\mathbf{E}\Big\{I_{l,j}^{(k)\,4}\Big\} + 6\sum_{k=2}^{K-1}\sum_{k'=k+1}^{K}\mathbf{E}\Big\{I_{l,j}^{(k)\,2}\Big\}\mathbf{E}\Big\{I_{l,j}^{(k')\,2}\Big\}. \tag{35}$$

Hence, it remains to evaluate the fourth order moment $\mathbf{E}\Big\{I_{l,j}^{(k)\,4}\Big\}$, which is shown to be

$$\mathbf{E}\Big\{I_{l,j}^{(k)\,4}\Big\} = \left(\frac{E_k}{E_1}\right)^2\left[\mathbf{E}\left\{\left[\sum_{l_1}a_{l_1}^{(k)}R_w\Big(\theta_{j',j}^{(k)}+(l_1-l)\Delta\Big)\right]^4\right\} + \mathbf{E}\left\{\left[\sum_{l_2}a_{l_2}^{(k)}R_w^2\Big(\theta_{j'-1,j}^{(k)}-T_f+(l_2-l)\Delta\Big)\right]^4\right\}\right] \tag{36}$$

because $|\theta_{j',j}^{(k)}-\theta_{j'-1,j}^{(k)}+T_f| \geq T_{mds}$ for $T_f \geq T_{mds}+N_hT_c$ and the cross-term becomes zero.

Similarly as in Appendix A, by taking the average with respect to the relative delays $\theta_{j',j}^{(k)}$ and $\theta_{j'-1,j}^{(k)}$, $\mathbf{E}\Big\{I_{l,j}^{(k)\,4}\Big\}$ can be evaluated as

$$\mathbf{E}\Big\{I_{l,j}^{(k)\,4}\Big\} = \left(\frac{E_k}{E_1}\right)^2\frac{1}{N_f}\sum_{n=-N_f}^{N_f-1}\frac{1}{T_c} \cdot\int_0^{T_c}\mathbf{E}\left\{\left[\sum_{m=0}^{N}a_{l-nN-m}^{(k)}R_w(\epsilon-m\Delta)\right]^4\right\}d\epsilon. \tag{37}$$

Due to zero-mean, uncorrelated channel gains across the MPCs, the above expectation becomes

$$\mathbf{E}\Big\{I_{l,j}^{(k)\,4}\Big\} = \left(\frac{E_k}{E_1}\right)^2\frac{1}{N_f}\sum_{n=-N_f}^{N_f-1}\left[\sum_{m=0}^{N}\mathbf{E}\Big\{\Big(a_{l-nN-m}^{(k)}\Big)^4\Big\}\varphi_m + 6\sum_{m=0}^{N-1}\sum_{m'=m+1}^{N}\mathbf{E}\Big\{\Big(a_{l-nN-m}^{(k)}\Big)^2\Big\} \cdot\mathbf{E}\Big\{\Big(a_{l-nN-m'}^{(k)}\Big)^2\Big\}\rho_{m,m'}\right] \tag{38}$$

where $\varphi_m = \mathbf{E}\{R_w^4(\epsilon-m\Delta)\}$ and $\rho_{m,m'} = \mathbf{E}\{R_w^2(\epsilon-m\Delta)R_w^2(\epsilon-m'\Delta)\}$. Therefore, upon substitution of $\mathbf{E}\Big\{I_{l,j}^{(k)\,4}\Big\}$ in (38) and $\mathbf{E}\Big\{I_{l,j}^{(k)\,2}\Big\}$ in (11) into (35) yields $\mathbf{E}\{I_{l,j}^4\}$ as given in (12).

APPENDIX C
PROOF OF PROPOSITION 4:

In the *discrete-time equivalent CIR* of (2), the composite channel gain $a_n^{(k)}$ denotes the sum of the channel gains of all the MPCs in nth time bin and this accounts for any possible *cluster overlapping*, often observed in the NLOS UWB channel models CM2, CM3 and CM4.

Let define

$$U_{n,q}^{(k)} = \begin{cases} 1, & \text{if the } q\text{th time bin has a MPC contribution to the } n\text{th time bin} \\ 0, & \text{otherwise,}\end{cases} \tag{39}$$

the composite channel gain $a_n^{(k)}$ is then expressed by

$$a_n^{(k)} = \sum_{q=0}^{n}p_{n,q}^{(k)}\,\beta_{n,q}^{(k)}\,U_{n,q}^{(k)} \tag{40}$$

where $\beta_{n,q}^{(k)}$ represents the MPC in nth time bin contributed by qth time bin, along with $p_{n,q}^{(k)}$ equiprobably taking on the values of ± 1. With this channel model, the fourth order moment of $a_n^{(k)}$ is formulated as

$$\begin{aligned}\mathbf{E}\Big\{a_n^{(k)\,4}\Big\} &= \mathbf{E}\left\{\left(\sum_{q=0}^{n}p_{n,q}^{(k)}\,\beta_{n,q}^{(k)}\,U_{n,q}^{(k)}\right)^4\right\} \qquad (n\geq 1)\\ &= \sum_{q=0}^{n}\mathbf{E}\Big\{\beta_{n,q}^{(k)\,4}\Big\}\Pr\Big[U_{n,q}^{(k)}=1\Big] + 6\sum_{q=0}^{n-1}\sum_{j=q+1}^{n}\mathbf{E}\Big\{\beta_{n,q}^{(k)\,2}\Big\}\mathbf{E}\Big\{\beta_{n,j}^{(k)\,2}\Big\} \cdot\Pr\Big[U_{n,q}^{(k)}=1,U_{n,j}^{(k)}=1\Big]\end{aligned} \tag{41}$$

where the probability of having $U_{n,q}^{(k)}=1$ is simply $P_q^{(n)}$, which is given by (16), and all the cross-terms of odd power disappear because of zero-mean, uncorrelated $p_{n,q}^{(k)}=\pm 1$.

Claim 1 : The probability of having both $U_{n,q}^{(k)}=1$ and $U_{n,j}^{(k)}=1$ $(q<j)$ is given by

$$\Pr\Big[U_{n,q}^{(k)}=1,U_{n,j}^{(k)}=1\Big] = P_q^{(n)}\cdot P_j^{(n)}. \tag{42}$$

Proof of claim 1: Case 1: for $1\leq q\leq n-2$ and $q<j\leq n-1$, the probability that both qth and jth time bins have

$$\begin{aligned}\Pr\left[U_{n,q}^{(k)}=1,U_{n,j}^{(k)}=1\right] &= \sum_{m=1}^{q}\Pr[T_m=qT_c]\sum_{m'=1}^{j-q}\Pr[T_{m'+m}=jT_c]\sum_{l=1}^{n-q}\Pr[\tau_{l,m}=(n-q)T_c]\sum_{l'=1}^{n-j}\Pr[\tau_{l',m'+m}=(n-j)T_c]\\ &= \sum_{m=1}^{q}\Pr[T_m=qT_c]\sum_{m'=1}^{j-q}\Pr[T_{m'+m}=jT_c]\sum_{l=1}^{n-q}P_r\binom{n-q-1}{l-1}P_r^{l-1}(1-P_r)^{n-q-l}\\ &\quad\cdot\sum_{l'=1}^{n-j}P_r\binom{n-j-1}{l'-1}P_r^{l'-1}(1-P_r)^{n-j-l'}\\ &= P_r^2\sum_{m=1}^{q}\Pr[T_m=qT_c]\sum_{m'=1}^{j-q}\Pr[T_{m'+m}=jT_c]\\ &= P_r^2\sum_{m=1}^{q}P_c\binom{q-1}{m-1}P_c^{m-1}(1-P_c)^{q-m}\sum_{m'=1}^{j-q}P_c\binom{j-q-1}{m'-1}P_c^{m'-1}(1-P_c)^{j-q-m'}\\ &= (P_cP_r)^2=P_q^{(n)}\cdot P_j^{(n)}\end{aligned}\tag{43}$$

their ray contributions to nth time bin can be derived as given in (43) at the top of next page.

Case 2: for $q=0$ and $1\le j\le n-1$, there is the first cluster ($m=0$) arrived in the zeroth ($q=0$) time bin with probability one, and hence

$$\begin{aligned}\Pr\left[U_{n,q}^{(k)}=1,U_{n,j}^{(k)}=1\right] &= \sum_{m'=1}^{j}\Pr[T_{m'}=jT_c]\\ &\quad\cdot\sum_{l=1}^{n}\Pr[\tau_{l,0}=nT_c]\sum_{l'=1}^{n-j}\Pr[\tau_{l',m'}=(n-j)T_c]\\ &= P_r\cdot(P_cP_r)=P_q^{(n)}\cdot P_j^{(n)}.\end{aligned}\tag{44}$$

Case 3: for $1\le q\le n-1$ and $j=n$,

$$\begin{aligned}\Pr\left[U_{n,q}^{(k)}=1,U_{n,j}^{(k)}=1\right] &= \sum_{m=1}^{q}\Pr[T_m=qT_c]\\ &\quad\cdot\sum_{m'=1}^{j-q}\Pr[T_{m'+m}=jT_c]\sum_{l=1}^{n-q}\Pr[\tau_{l,m}=(n-q)T_c]\\ &= (P_cP_r)\cdot P_c=P_q^{(n)}\cdot P_j^{(n)}.\end{aligned}\tag{45}$$

Note that the probability $P_j^{(n)}$ here is equivalent to the probability of a cluster arrival, which is P_c.

Case 4: for $q=0$ and $1\le j=n$,

$$\begin{aligned}&\Pr\left[U_{n,q}^{(k)}=1,U_{n,j}^{(k)}=1\right]\\ &= \sum_{m'=1}^{j}\Pr[T_{m'}=jT_c]\sum_{l=1}^{n}\Pr[\tau_{l,0}=nT_c]\\ &= P_r\cdot P_c=P_q^{(n)}\cdot P_j^{(n)}.\end{aligned}\tag{46}$$

■

According to the IEEE 802.15.3a channel model [15], the channel gain $\beta_{n,q}^{(k)}$ follows the lognormal distribution, namely $20\log_{10}(\beta_{n,q}^{(k)})\propto N(\mu_{n,q},\sigma^2)$, where the mean is given by $\mu_{n,q}=\xi\left[\ln(\Omega_0)-qT_c/\Gamma-(n-q)T_c/\gamma\right]-\sigma^2/2\xi$ and the mth order moment is evaluated as

$$\mathbf{E}\left\{\beta_{n,q}^{(k)\,2m}\right\}=\exp\left(\frac{m\mu_{n,q}}{\xi}+\frac{m^2\sigma^2}{2\xi^2}\right).\tag{47}$$

Therefore, substituting (47) with $m=1,2$ and (42) into (41) along with $\Pr\left[U_{n,q}^{(k)}=1\right]=P_q^{(n)}$ produces (15).

APPENDIX D
PROOF OF PROPOSITION 5:

The second order moment of $\tilde{I}_j=\sum_{l=0}^{L_p-1}a_l^{(1)}I_{l,j}$ is easily obtained as

$$\mathbf{E}\{\tilde{I}_j^2\}=\sum_{l=0}^{L_p-1}\mathbf{E}\left\{a_l^{(1)^2}\right\}\mathbf{E}\{I_{l,j}^2\}\tag{48}$$

because the channel gains $\{a_l^{(1)}\}$ are zero-mean, uncorrelated across the MPCs. Hence, combining this with (11) gives (25).

Next, the fourth order moment of $\tilde{I}_j$ can be written as

$$\begin{aligned}\mathbf{E}\{\tilde{I}_j^4\} &= \sum_{l=0}^{L_p-1}\mathbf{E}\left\{a_l^{(1)^4}\right\}\mathbf{E}\{I_{l,j}^4\}\\ &\quad+6\sum_{l=0}^{L_p-2}\sum_{l'=l+1}^{L_p-1}\mathbf{E}\left\{a_l^{(1)^2}\right\}\mathbf{E}\left\{a_{l'}^{(1)^2}\right\}\mathbf{E}\left\{I_{l,j}^2I_{l',j}^2\right\}.\end{aligned}\tag{49}$$

Since there exists non-zero correlation between $I_{l,j}$ and $I_{l',j}$ when $l'=l\pm1$, but it can be ignored because of $\mathbf{E}\{R_w(\epsilon)R_w(T_c-\epsilon)\}\cong0$, the expectation $\mathbf{E}\left\{I_{l,j}^2I_{l',j}^2\right\}$ can be approximated to

$$\begin{aligned}\mathbf{E}\left\{I_{l,j}^2I_{l',j}^2\right\} &\cong \sum_{k=2}^{K}\mathbf{E}\left\{I_{l,j}^{(k)^2}I_{l',j}^{(k)^2}\right\}\\ &\quad+2\sum_{k=2}^{K-1}\sum_{k'=k+1}^{K}\mathbf{E}\left\{I_{l,j}^{(k)^2}\right\}\mathbf{E}\left\{I_{l',j}^{(k')^2}\right\}.\end{aligned}\tag{50}$$

It remains to evaluate the expectation $\mathbf{E}\left\{I_{l,j}^{(k)^2}I_{l',j}^{(k)^2}\right\}$, which is similarly approximated to

$$\begin{aligned}\mathbf{E}\left\{I_{l,j}^{(k)^2}I_{l',j}^{(k)^2}\right\} &\cong \left(\frac{E_k}{E_1}\right)^2\frac{1}{N_f}\sum_{n=-N_f}^{N_f-1}\frac{1}{T_c}\\ &\quad\cdot\int_0^{T_c}\mathbf{E}\left\{\left[a_{l-n}^{(k)}R_w(\epsilon)+a_{l-n-1}^{(k)}R_w(T_c-\epsilon)\right]^2\right.\\ &\quad\left.\cdot\left[a_{l'-n}^{(k)}R_w(\epsilon)+a_{l'-n-1}^{(k)}R_w(T_c-\epsilon)\right]^2\right\}d\epsilon.\end{aligned}\tag{51}$$

Again, because of $\mathbf{E}\{R_w^2(\epsilon)R_w^2(T_c-\epsilon)\} \cong 0$, it can be further approximated to

$$\mathbf{E}\left\{ {I_{l,j}^{(k)}}^2 {I_{l',j}^{(k)}}^2 \right\} \cong \left(\frac{E_k}{E_1}\right)^2 \frac{1}{N_f} \sum_{n=-N_f}^{N_f-1} \frac{1}{T_c} \cdot \int_0^{T_c} \left[\mathbf{E}\left\{ {a_{l-n}^{(k)}}^2 \right\} \mathbf{E}\left\{ {a_{l'-n}^{(k)}}^2 \right\} R_w^2(\epsilon) + \mathbf{E}\left\{ \left(a_{l-n-1}^{(k)}\right)^2 \right\} \mathbf{E}\left\{ \left(a_{l'-n-1}^{(k)}\right)^2 \right\} R_w^2(T_c-\epsilon) \right] d\epsilon. \quad (52)$$

Now, combining the above results with (11) and (12) yields (26).

REFERENCES

[1] IEEE 802.15.4a, Low rate alternative PHY task group (TG4a) for wireless personal area networks. [Online.] Available: http://ieee802.org/15.

[2] R. A. Scholtz, "Multiple access with time-hopping impulse modulation," in *Proc. IEEE MILCOM '93*, pp. 447-450, Oct. 1993.

[3] M. Z. Win and R. A. Scholtz, "Ultra-wide bandwidth time-hopping spread-spectrum impulse radio for wireless multiple-access communications," *IEEE Trans. Commun.*, vol. 48, pp. 679-691, Apr. 2000.

[4] G. Durisi and S. Benedetto, "Performance evaluation of TH-PPM UWB systems in the presence of multiuser interference," *IEEE Commun. Lett.*, vol. 7, pp. 224-226, May 2003.

[5] A. R. Forouzan, M. Nasiri-Kenari, and J. A. Salehi, "Performance analysis of time-hopping spread-spectrum multiple-access systems: uncoded and coded schemes," *IEEE Trans. Wireless Commun.*, vol. 1, pp. 671-681, Oct. 2002.

[6] B. Hu and N. C. Beaulieu, "Exact bit error rate analysis of TH-PPM UWB systems in the presence of multiple-access interference," *IEEE Commun. Lett.*, vol. 7, pp. 572-574, Dec. 2003.

[7] B. Hu and N. C. Beaulieu, "Accurate evaluation of multiple-access performance in TH-PPM and TH-BPSK UWB systems," *IEEE Trans. Commun.*, vol. 52, pp. 1758-1766, Oct. 2004.

[8] B. Hu and N. C. Beaulieu, "Accurate performance evaluation of time-hopping and direct-sequence UWB systems in multi-user interference," *IEEE Trans. Commun.*, vol. 53, pp. 1053-1062, June 2005.

[9] N. C. Beaulieu and S. Niranjayan, "New UWB receiver designs based on a Gaussian-Laplacian noise-plus-MAI model," in *Proc. IEEE ICC '07*, Glasgow, Scotland, UK, June 2007.

[10] N. C. Beaulieu and B. Hu, "A soft-limiting receiver structure for time-hopping UWB in multiple access interference," in *Proc. IEEE ISSSTA '06*, pp. 417-421, Aug. 2006.

[11] J. Fiorina, "A simple IR-UWB receiver adapted to multi-user interferences," in *Proc. IEEE GLOBECOM '06*, San Francisco, CA, Nov. 2006.

[12] T. Erseghe, V. Cellini, and G. Dona, "UWB impulse radio receivers derived from a Gaussian mixture interference model," in *Proc. IEEE ICC '07*, Glasgow, Scotland, UK, June 2007.

[13] B. S. Kim, J. Bae, I. Song, S. Y. Kim, and H. Kwon, "A comparative analysis of optimum and suboptimum rake receivers in impulsive UWB environment," *IEEE Trans. Veh. Technol.*, vol. 55, pp. 1797-1804, Nov. 2006.

[14] N. C. Beaulieu, H. Shao, and J. Fiorina, "P-order metric UWB receiver structures with superior performance," *IEEE Trans. Commun.*, vol. 56, pp. 1666-1676, Oct. 2008.

[15] A. F. Molisch, J. R. Foerster, and M. Pendergrass, "Channel models for ultrawideband personal area networks," *IEEE Personal Commun. Mag.*, vol. 10, pp. 14-21, Dec. 2003.

[16] S. M. Kay, *Fundamentals of Statistical Signal Processing: Detection Theory*. Englewood Cliffs, NJ: Prentice Hall, 1998.

[17] H. Mathis, "Nonlinear functions for blind separation and equalization," Ph.D. thesis, Swiss Federal Institute of Technology, Zurich, Switzerland, Nov. 2001.

[18] T. Jia and D. I. Kim, "Analysis of average signal-to-interference-noise ratio for indoor UWB rake receiving system," in *Proc. IEEE VTC Spring '05*, vol. 2, pp. 1396-1400, Stockholm, Sweden, May 2005.

[19] T. Erseghe, V. Cellini, and G. Dona, "On UWB impulse radio receivers derived by modeling MAI as a Gaussian mixture process," *IEEE Trans. Wireless Commun.*, vol. 7, pp. 2388-2396, June 2008.

[20] Y. Chen and N. C. Beaulieu, "Improved receivers for generalized UWB transmitted reference systems," *IEEE Trans. Wireless Commun.*, vol. 7, pp. 500-504, Feb. 2008.

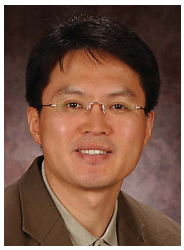

Dong In Kim (S'89-M'91-SM'02) received the B.S. and M.S. degrees in Electronics Engineering from Seoul National University, Seoul, Korea, in 1980 and 1984, respectively, and the M.S. and Ph.D. degrees in Electrical Engineering from University of Southern California (USC), Los Angeles, in 1987 and 1990, respectively.

From 1984 to 1985, he was a Researcher with Korea Telecom Research Center, Seoul. From 1986 to 1988, he was a Korean Government Graduate Fellow in the Department of Electrical Engineering, USC. From 1991 to 2002, he was with the University of Seoul, Seoul, leading the Wireless Communications Research Group. From 2002 to 2007, he was a tenured Full Professor in the School of Engineering Science, Simon Fraser University, Burnaby, BC, Canada. From 1999 to 2000, he was a Visiting Professor at the University of Victoria, Victoria, BC. Since 2007, he has been with Sungkyunkwan University (SKKU), Suwon, Korea, where he is a Professor and SKKU Fellow in the School of Information and Communication Engineering. Since 1988, he is engaged in the research activities in the areas of wideband wireless transmission and access. His current research interests include cooperative relaying and base station (BS) cooperation, multiuser cognitive radio networks, advanced transceiver design, and cross-layer design.

Dr. Kim was an Editor for the IEEE JOURNAL ON SELECTED AREAS IN COMMUNICATIONS: WIRELESS COMMUNICATIONS SERIES and also a Division Editor for the JOURNAL OF COMMUNICATIONS AND NETWORKS. He is currently an Editor for Spread Spectrum Transmission and Access for the IEEE TRANSACTIONS ON COMMUNICATIONS and an Area Editor for Transmission Technology III for the IEEE TRANSACTIONS ON WIRELESS COMMUNICATIONS. He also serves as Co-Editor-in-Chief for the JOURNAL OF COMMUNICATIONS AND NETWORKS.